Study on Crawler-Type Solar EV

Toru Fujisawa[1], Yuki Nemoto[1], and Takashi Kawaguchi[1]

[1] Kanagawa Institute of Technology, Atsugi (Japan)

Abstract

In this study, a photovoltaic module was installed on the rooftop of a crawler vehicle. If the power grid is unable to supply electricity, the crawler-type solar electric vehicle (solar EV) is able to travel on rough ground and has a self-charging function owing to solar energy absorption. The crawler can move in various ground conditions, such as asphalt, soil, grass, and gravel. Driving experiments were performed under different conditions, and we measured the photovoltaic current, voltage, acceleration, and power consumption. As a result, the solar fraction is compared with the vibration, it was found that solar fraction of the crawler-type solar EV was achieved 40-44 % on a winter clear day, power consumption of the motor was not proportional to z-axis acceleration. For specified solar fraction, ratio between PV and motor ratings was around 30 %, it is larger than scooter-type solar EV.

Keywords: Crawler, Solar EV, PV System, Solar Fraction, Farm Car

1. Introduction

After the Great East Japan Earthquake of 2011, as damaged infrastructure needed a longer time to return to a normal state, many Japanese people considered harvesting solar energy for daily life, and also for automobile use. Solar EV is a unique name proposed by the regulation of the World Solar Challenge (WSC 2012). In Japan, a company (Fukuzawa-Oder, 2015) produced a crawler-type solar-power-driven planter for Chinese yams (*Dioscorea batatas*). In recent years, we found the motivation for this study from our university students, aiming at developing sustainable solar-powered EV. It is a low-cost and reusable vehicle with potential applications in areas such as agriculture, delivery use (Toru Fujisawa and Takashi Kawaguchi, 2016), on uneven surfaces, or in rural areas with a stand-alone photovoltaic system.

2. EV conversion

The solar EV is converted from an old grain thresher, OSHIMA Harvester MK-100 (fabricated by Oshimanoki, 1983–1986), as shown in Fig. 1. Its driving seat and photovoltaic module are reused components. The aluminum frame, synchronous motor, lead-acid battery, inverter, and boost-type maximum power point tracker (MPPT) are new components needed for conversion to a solar EV. Tab. 1 gives the specifications of the grain threshing machine. Tab. 2 lists the major components of the converted crawler-type solar EV. Fig. 2 shows a side view of the crawler-type solar EV. In the figure, each major component is indicated. The electrical system of the crawler-type solar EV is shown in Fig. 3.

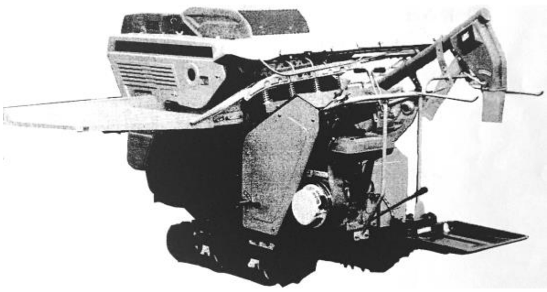

Fig. 1: Oshima MK-100 thresher

doi:10.18086/swc.2017.20.01 Available at http://proceedings.ises.org

Tab. 1: Specifications of the grain thresher

Length	**Width**	**Height**	**Tread**	**Mass**
1,743 mm	878 mm	1,586 mm	635 mm	181 kg
Max speed of powertrain	**Max Engine Power**	**Engine**	**Compression Ratio**	**Fuel**
1,800 rpm	3.5 PS	G510L NA 192 cc	6.2	Unleaded petrol

The traveling speed of the thresher can be selected, at 0.38 m/s, 0.43 m/s, and 0.91 m/s, using its transmission gear. We considered traveling safety and decided to avoid using a highest-speed gear. When the engine pulley rotates 10 rounds in the lowest gear, the crawler travels 1.2 m on the road. This means that the vehicle speed can be calculated from the rpm of the driving unit.

Tab. 2: Specifications of major components for converted crawler-type Solar EV

Battery	**Motor**	**Inverter**	**PV module**	**Tracker**	**Pyranometer**
VRLA 12 V × 4, 20 Ah	FBLM86 PMSM 660 W	BLD4820 ≤ 1200 W	MD-HH210T 210 W	Boost PT-209U	Silicon sensor ML-020VM

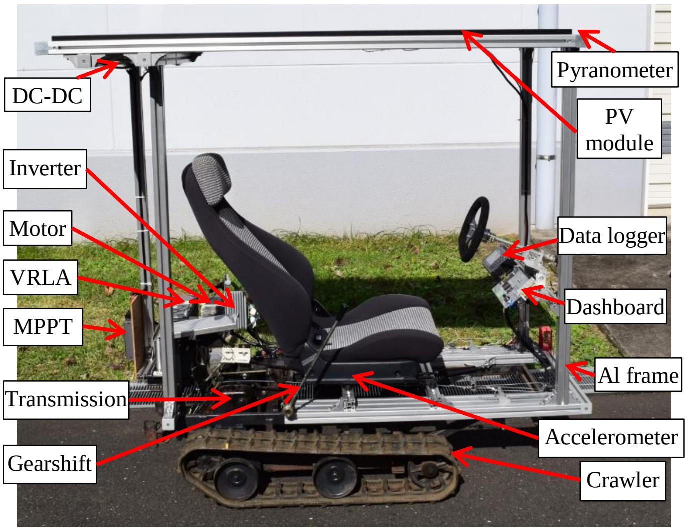

Fig. 2: Crawler-type Solar EV

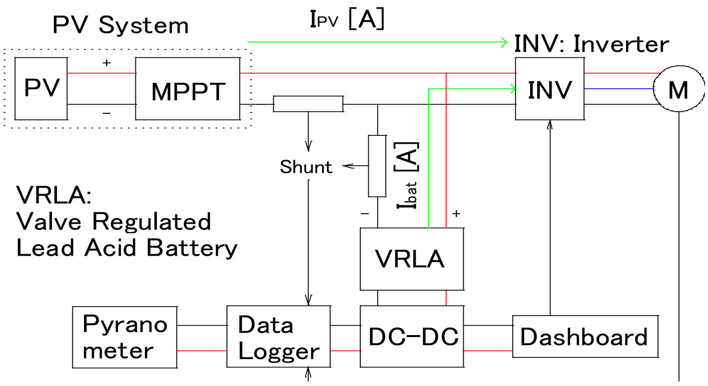

Fig. 3: Block diagram of electrical system

Fig. 4 shows outdoor solar charging in summer and an indoor garage view with undergraduate students in winter. Fig. 5 represents the PV system output current, valve regulated lead acid (VRLA) battery current, and motor current while climbing backward a step from asphalt to greenbelt ground, as in Fig. 4.

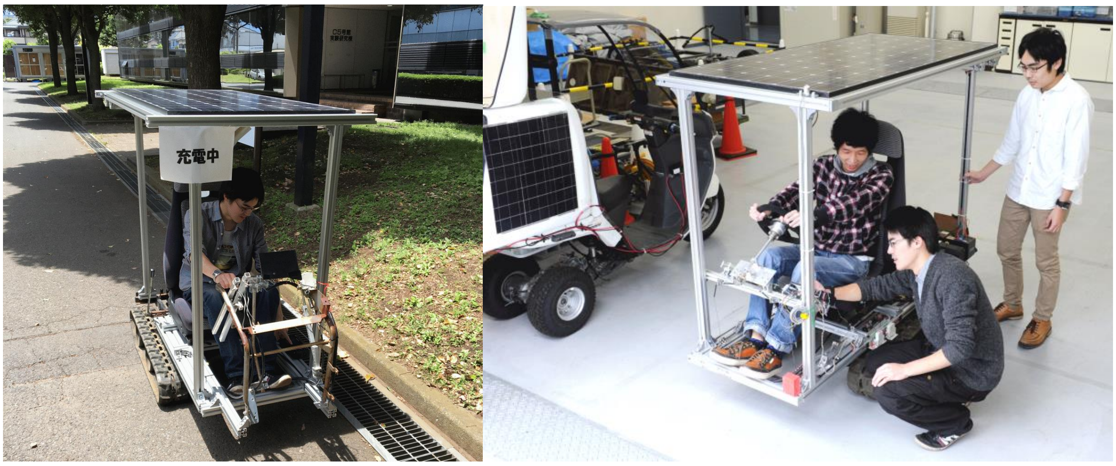

Fig. 4: Converted crawler-type solar EV (Left: outdoor charging in summer, Right: in a garage in winter)

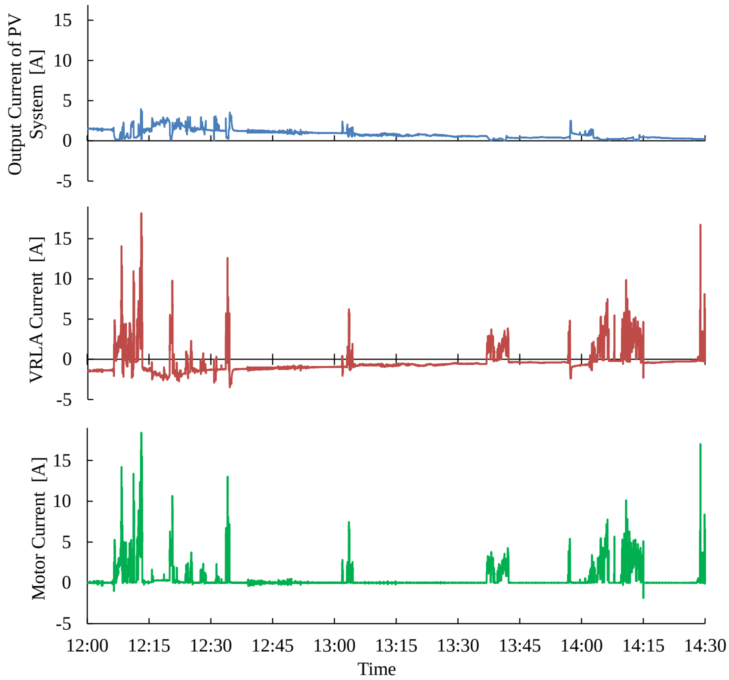

Fig. 5: Motor current and PV system output current in summer (climbing backward a step from asphalt to greenbelt ground)

3. Evaluations

3.1. Solar Fraction

The solar fraction (F_s) was calculated using the output PV power (P_{pv}) and consumed power using load (P_{load}).

$$F_s = \frac{\int P_{pv} dt}{\int P_{load} dt} \qquad \text{(eq. 1)}$$

$$P_{pv} = I_{pv} V_{bat} \qquad \text{(eq. 2)}$$

$$P_{load} = I_{bat} V_{bat}, \qquad \text{(eq. 3)}$$

Here, I_{pv} is the output current of the peak power tracker, V_{bat} is the voltage of the lead-acid battery (same as the load voltage), and I_{bat} is the current of the battery. These data, along with the irradiance, accelerometer output, and revolution speed (12 pulses per revolution) of the motor are recorded by a 10-channel data-logger (GRAPHTECH GL220A) every 100 ms.

A three-axis accelerometer, Kionix KXSC7-2050, was installed under the driving seat near the center of mass, as shown in Fig. 6. The output from this sensor is also recorded simultaneously in the same interval by the logger. To evaluate the vibration of the vehicle, the root mean square (RMS) value of the z-axis acceleration a_z is calculated as

$$RMSA = \sqrt{\frac{\sum_{i=1}^{n} {a_{z_i}}^2}{n}}. \qquad \text{(eq. 4)}$$

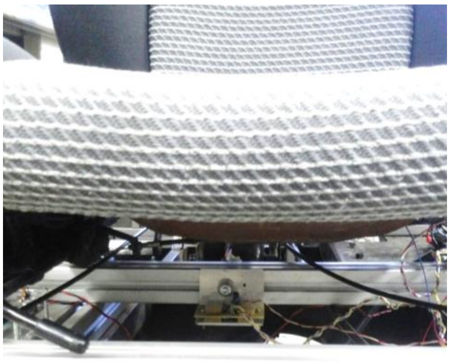

Fig. 6: Installation position of three-axis accelerometer

3.2. Experiments

Three different experimental surfaces are shown in Fig. 7. The grain diameter of gravel was ~15–40 mm, and the glass depth was ~20–40 mm. The experimental results of speed vs. power consumption on the three different surfaces, gravel, grass, and asphalt, are shown in Fig. 8. Fig. 9 shows the z-axis acceleration for the RMS value vs. vehicle speed. From this figure and the previous one, it can be observed that the z-axis acceleration does not always directly affect the power consumption of the driving load.

(a) gravel **(b) glass** **(c) asphalt**

Fig. 7: Ground surface conditions

As a result, the power consumption was greater on gravel and glass than on asphalt. On the other hand, the RMS value of the z-axis acceleration is smaller on grass and on asphalt than that on gravel. The solar fraction for each condition is calculated using eq. 1 and listed in Tab. 3.

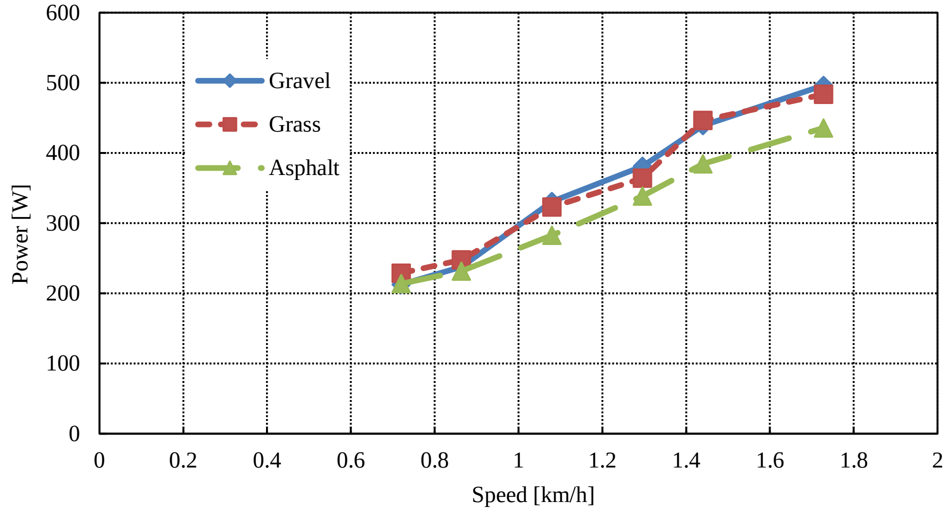

Fig. 8: Speed vs. average power consumption for three different roads

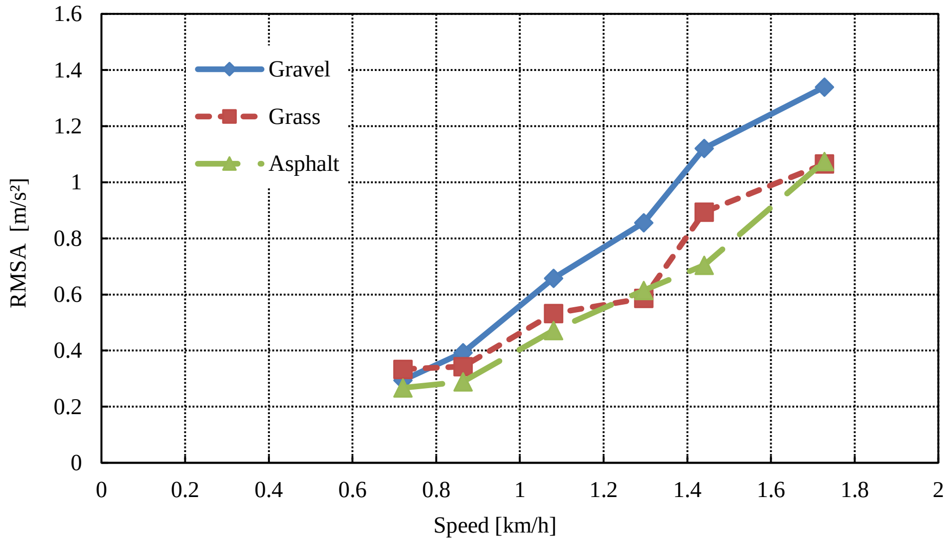

Fig. 9: RMS acceleration of vertical direction (z-axis) vs. vehicle speed

Tab. 3: Solar fraction of crawler-type solar EV on different flat surfaces on a clear winter day

Motor Speed	**Gear**	**Speed [km h^{-1}]**	**Gravel 15th Dec 17**	**Grass 26th Jan 17**	**Asphalt 21st Jan 17**
1000 [rpm]	First	0.720	60.9 %	56.6 %	60.6 %
	Second	0.864	54.5 %	52.3 %	55.9 %
1500 [rpm]	First	1.08	39.2 %	40.1 %	45.8 %
	Second	1.30	34.0 %	35.6 %	38.3 %
2000 [rpm]	First	1.44	29.5 %	29.0 %	33.7 %
	Second	1.73	26.1 %	26.8 %	29.7 %
Average			40.7 %	40.1 %	44.0 %
Peak Irradiance [W/m^2]			645	527	637
Solar Altitude [deg.]			30.9	25.9	34.8

4. Discussions

Tab. 4 presents the comparison between various solar EVs. The power unit, mass, PV rating, battery capability, travel distance per charge, and solar mileage are discussed. Fig. 10 shows the ratio between the PV and power unit ratings in terms of the specified solar fraction for comparison. Spirit is the name of the racing solar car that participated in the WSC 2013 Adventure class, the Gyro Canopy is a converted solar EV scooter, and the Prius PHV is TOYOTA's first commercial solar EV that can incorporate electric power into its power battery storage while driving.

Tab. 4: Three different types of Solar EV and plug-in HEV with photovoltaic roof (including 60-kg driver)

	Motor	Mass	PV	Motor / Mass	Battery	PV / Motor	Distance	Solar mileage	Duration
	[kW]	[kg]	[kW]	[W/kg]	[kWh]	[-]	[km/charge]	[km/day]	[h]
Racing solar car KAIT Spirit	2.0	220	1.3	9.52	5.0	0.65	350	300	4.3
Crawler solar EV	0.66	245	0.21	2.69	0.6	0.32	1.5	0.6	0.6
Gyro canopy converted solar EV	1.5	210	0.13	7.14	1.3	0.87	19.5	2.4	0.2
Prius PHV	80	1810	0.2	44.2	10	0.0025	60	6	0.1

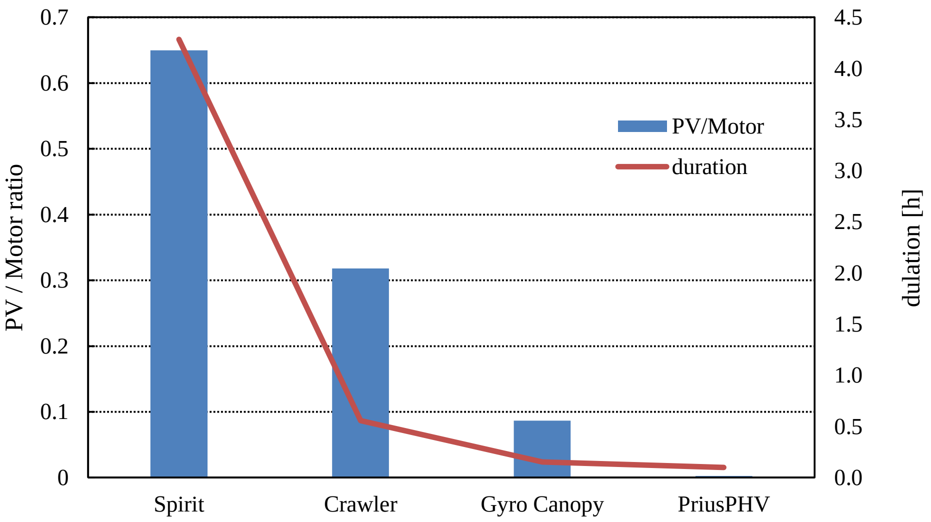

Fig. 10: The ratio between PV and power ratings

5. Conclusions

From the outdoor driving experiments with the converted crawler-type solar EV, the following conclusions were drawn:

- The solar fraction was 44% on the asphalt road on a sunny winter day.
- The consumed power was proportional to the vehicle speed, and the lowest curve was obtained on an asphalt road.
- The crawler-type solar EV is affordable with a 660-W synchronous motor and a VRLA battery with a nominal power of 48 V.
- The highest power consumption rate was obtained on asphalt, achieving 10 km/kWh in the lowest gear.
- The rating power ratio of PV/Motor for the crawler-type solar EV was 0.32.

Farm-use cars or robotic vehicles are necessary for Japanese rural agriculture, as the rapidly aging society with fewer children has become the largest problem for Japan's future.

6. References

Fukuzawa-Order, 2015, Solar Nagaimo Planter, fukuzawa-order.com (last access: 14 OCT 2017)

Oshimanoki, 1983, MK-100 User's manual, www.oshimanoki.com (last access: 14 OCT 2017)

Toru Fujisawa and Takashi Kawaguchi, EuroSun 2016, Performance Evaluation and Trial Making of a Compact Solar EV, No. 0134, ISES Conference Proceedings, DOI:10.18086/eurosun.2016.08.05

World Solar Challenge, 2012, World Solar Challenge Regulations, www.worldsolarchallenge.org (last access: 19 JUN 2012).